LogLinear Group

Single Beam WiPPR

Marshall Bradley and Mark Henderson
December 2021

The results presented here grew out of the time period (2011-2013) in which the Wind Profiling Portable Radar (WiPPR) system collected and stored real time FMCW data. This made it possible to form radar data cubes in Doppler Velocity/slow time /slant range (VTR) and to track clear air particles as they moved through the radar beam. A study of the characteristics of these particle tracks led to the idea of estimating wind speed and direction from a single beam. The single beam approach can be used in situations, e.g. canyons, where it is not possible to employ the four-directional beam approach. Results from the original analyses conducted during that time period and a detailed review of the single beam idea in 2016 are summarized and presented here.

Clear air scatter contacts when viewed in Doppler velocity-slow time space usually appear to accelerate away regardless of their Doppler velocity. Why is this?

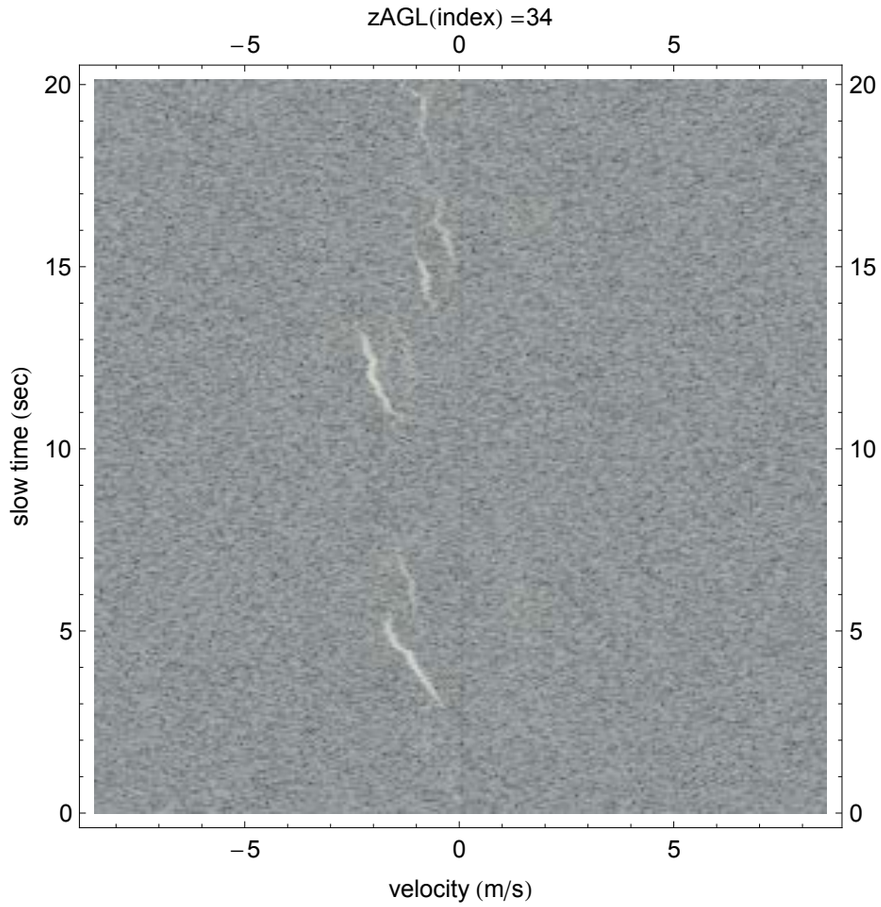

Figure 1. Clear air scatter particles moving through the WiPPR data cube at an altitude of about 100 m. Horizontal axis is Doppler velocity. Vertical axis is slow time. Data recorded in March 2012 at Yuma AZ. The figure is a slice of a VTR data cube at a fixed slant range. Contacts appear to accelerate away moving from higher to lower Doppler velocity.

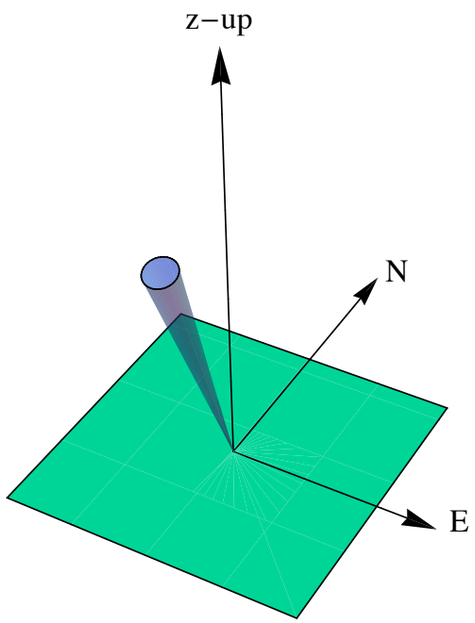

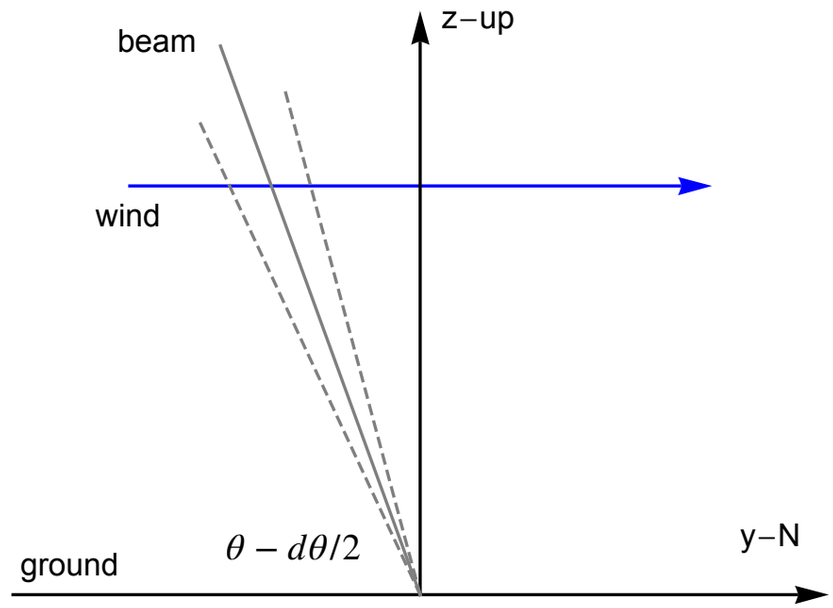

Figure 2. Single beam radar geometry. Left) South pointing radar beam. Right) Particle coming from the south. The beam pointing direction is $\boldsymbol{\eta} = (0, -\cos(\theta), \sin(\theta))$. *The vector velocity of the particle is* $\mathbf{v}_{wind} = (0,v,0)$. *The mid-crossing Doppler velocity is* $V = -\boldsymbol{\eta} \cdot \mathbf{v}_{wind} = v\cos(\theta)$. *The particle first appears at Doppler velocity* $v\cos(\theta - d\theta/2)$ *and exits at Doppler velocity* $v\cos(\theta + d\theta/2)$. *The change in Doppler velocity is* $-v\sin(\theta)d\theta$. *This is negative and the particle will appear to accelerate away when viewed in VT space as shown in the previous figure. A negative change in Doppler leads to a negative apparent acceleration.*

To see this, we begin with an example and then generalize. Consider a south pointing radar beam inclined up from the horizontal at angle θ. The lower edge of the beam is at angle $\theta - d\theta/2$ with respect to the horizontal as shown in figure 2. The pointing direction of the beam center in is $\boldsymbol{\eta} = (0, -\cos(\theta), \sin(\theta))$. Now consider a wind particle coming from the south with velocity $\mathbf{v} = (0,v,0)$. The mid-crossing Doppler velocity observed by the radar is $V = -\boldsymbol{\eta} \cdot \mathbf{v}$. If $d\theta$ denotes the angular width of the beam, then the particle will enter the beam with Doppler velocity $V_1 = v\cos(\theta - d\theta/2)$ and exit the beam at Doppler velocity $V_2 = v\cos(\theta + d\theta/2)$. The change in Doppler velocity is

$$dV = V_2 - V_1 = -2v\sin(\theta)\sin(d\theta/2) = -v\sin(\theta)d\theta$$

for small $d\theta$. If the direction of particle motion is reversed, i.e. if the particle is coming from the north, the exact same result is obtained. This suggests that the change in Doppler velocity might be independent of wind direction for a near vertical radar beam.

A more detailed kinematic explanation proceeds as follows. In general the radar beam will point in the direction $\boldsymbol{\eta} = (\sin(\phi)\cos(\theta), \cos(\phi)\cos(\theta), \sin(\theta))$ and the hot spot of the radar beam corresponding to slant range r will be located at the point $\mathbf{r}_{hot} = r(\sin(\phi)\cos(\theta), \cos(\phi)\cos(\theta), \sin(\theta))$. At time t the wind particle will be located at $\mathbf{r}_{wind}(t) = vt(\sin(\psi), \cos(\psi),0)$ where v is the wind speed (not velocity) and ψ is the direction the wind is coming from. All kinematic quantities of interest related to wind particle motion relative to the pointing direction of the radar beam can be obtained from the path length from the radar location to the wind particle. This is $R(t) = |\,\mathbf{r}_{hot} - \mathbf{r}_{wind}(t)\,|^{1/2}$ which can be shown to be

$$R(t) = \sqrt{r^2 + 2rtv\cos(\theta)\cos(\phi - \psi) + t^2v^2}$$

The Doppler shift is $V = -\,dR(t)/dt$ which is

$$V(t) = -\frac{v(r\cos(\theta)\cos(\phi - \psi) + tv)}{\sqrt{r^2 + 2rtv\cos(\theta)\cos(\phi - \psi) + t^2v^2}}$$

A time $t = 0$ when the particle goes through the beam hot spot the Doppler shift is

$$V = -\,v\cos(\theta)\cos(\phi - \psi)$$

and the acceleration $\alpha = dV/dt$ is

$$\alpha = \frac{v^2\left(2\cos^2(\theta)\cos(2(\phi - \psi)) + \cos(2\theta) - 3\right)}{4r}$$

For near vertical angles ($\theta = \pi/2$) the acceleration simplifies to

$$\alpha = -\frac{v^2}{r}$$

Thus if we can measure the acceleration α of a particle as it passes through the radar beam, we can infer the wind speed from

$$v = -\,(-\alpha r)^{1/2}.$$

If the wind speed is determined by the above relationship then we can infer the wind direction ψ from

$$\psi = \phi \pm \arccos\left(\frac{-V}{(-\alpha r)^{1/2}\cos(\theta)}\right)$$

This last equation determines wind direction with respect to azimuthal beam direction. The $\pm$ sign arrises in the equation due to the even nature of the cosine function.

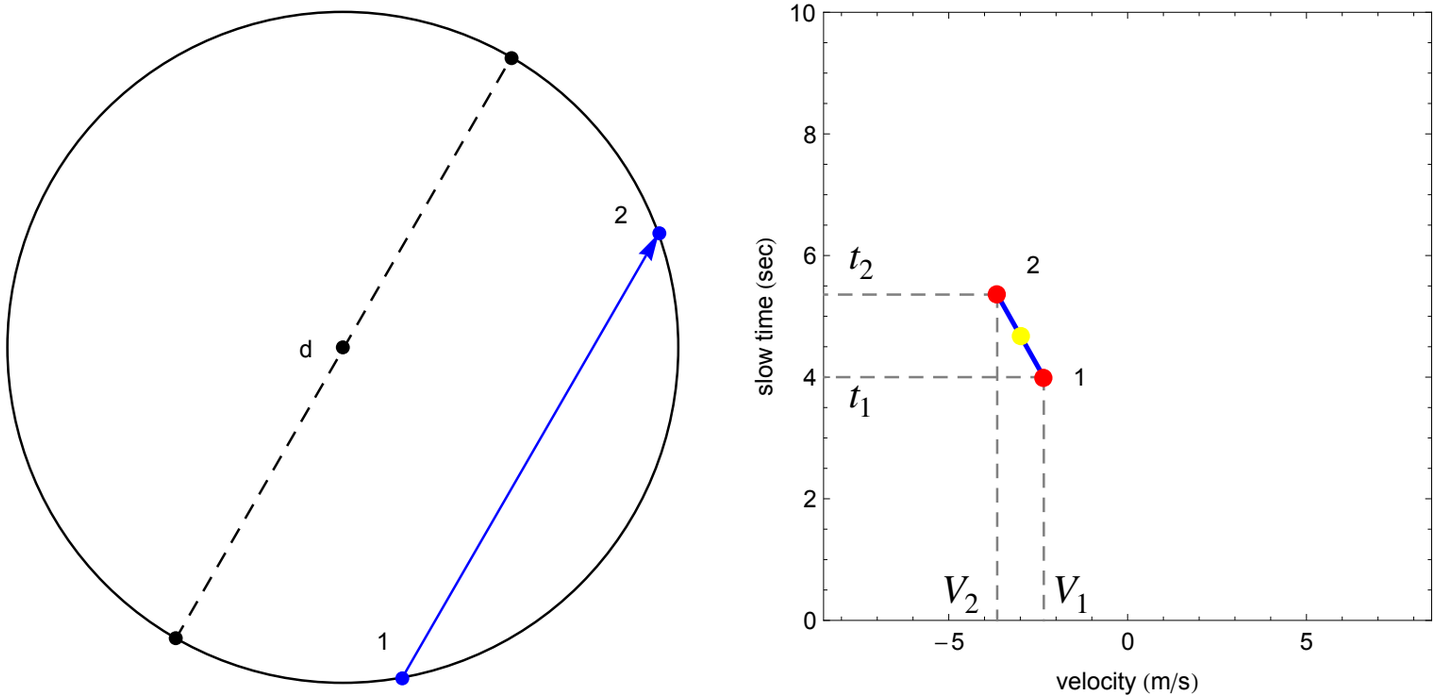

Figure 3. Left) Bird's eye view of particle crossing radar beam spot. The diameter if the spot is $d = rd\theta$. The particle particle crossing as indicated on the blue dotted line form 1 to 2. Right) Particle kinematics in Doppler velocity-slow time gram.

From a single beam measurement we can infer the wind velocity v and the relative wind direction ψ provided we can measure Doppler velocity V and Doppler acceleration α as well as the slant range r of the contact. This is the essence of the single beam method for determining wind velocity from a radar that employs a single, non-rotating beam.

With reference to figure 3, the acceleration of the particle is

$$\alpha = \frac{V_2 - V_1}{t_2 - t_1}$$

This quantity is less than zero as drawn.

An interesting aspect of the acceleration is that it is distinctly larger in magnitude at lower altitudes than at higher as shown in

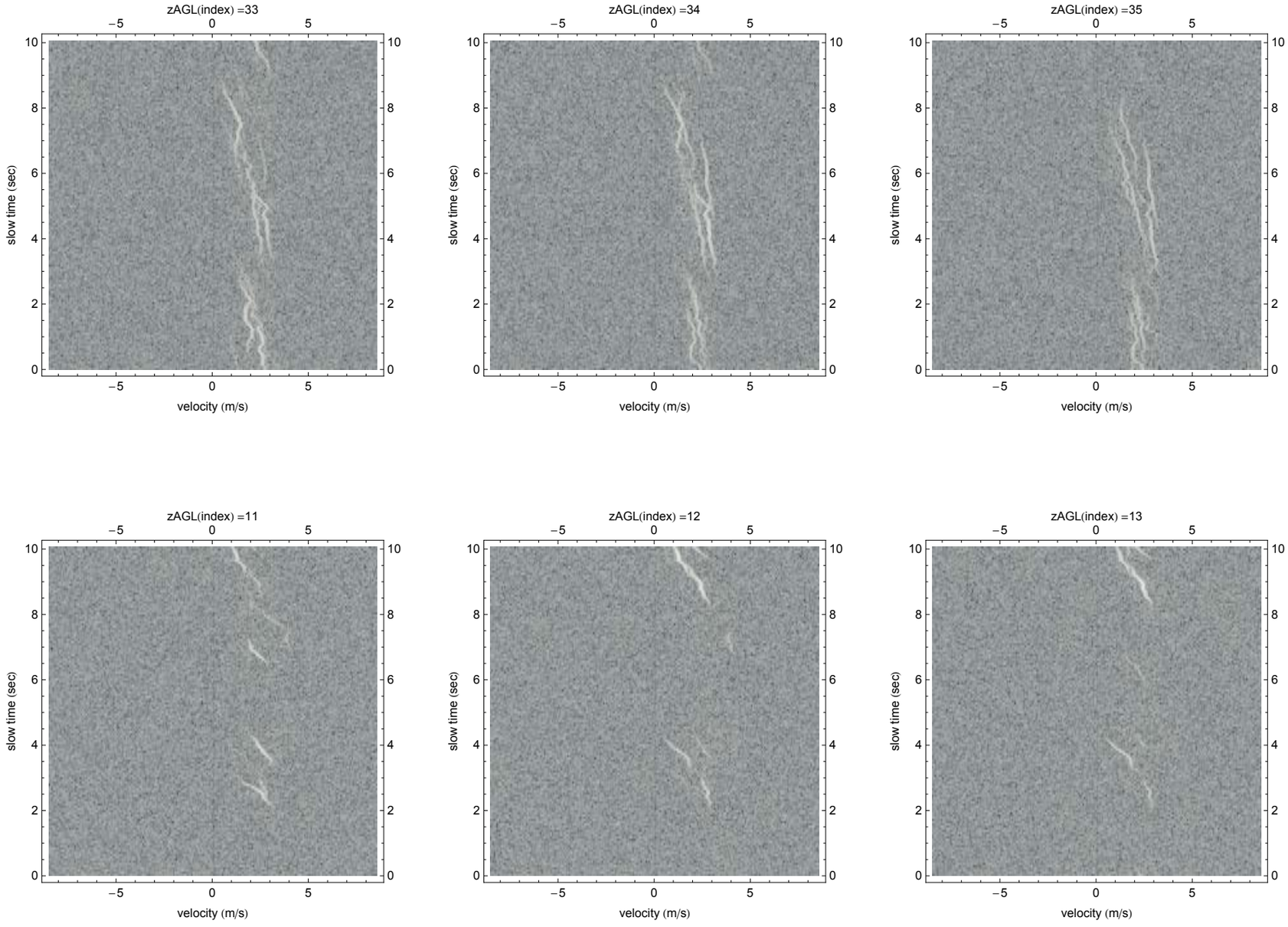

Figure 4. Variation of turbulent feature crossing times with altitude. Lower) Altitude index 11-13 (r is 34-41 m). Beam diameters are small so particles cross quickly and accelerations are large. Upper),Altitude index 33-35 (r is 103-109 m). Beam diameters are larger so particles cross more slowly and accelerations are smaller.

figure 4. This is because crossing times are smaller at the lower altitudes. This follows from the fact that the beam diameter is approximately for a near vertical beam $d = rd\theta$ and $t_2 - t_1 = rd\theta/v$ which decreases with r. On the other hand $V_2 - V_1 = -vd\theta$ which is independent of the slant range r.

Particle crossing phenomena tend to repeat across about 3 slant range cells as shown in figure 5. This may simply be a direct result of spectral leakage in the fast-time, slow-time image forming process used to created the individual range velocity matrices in a data cube.

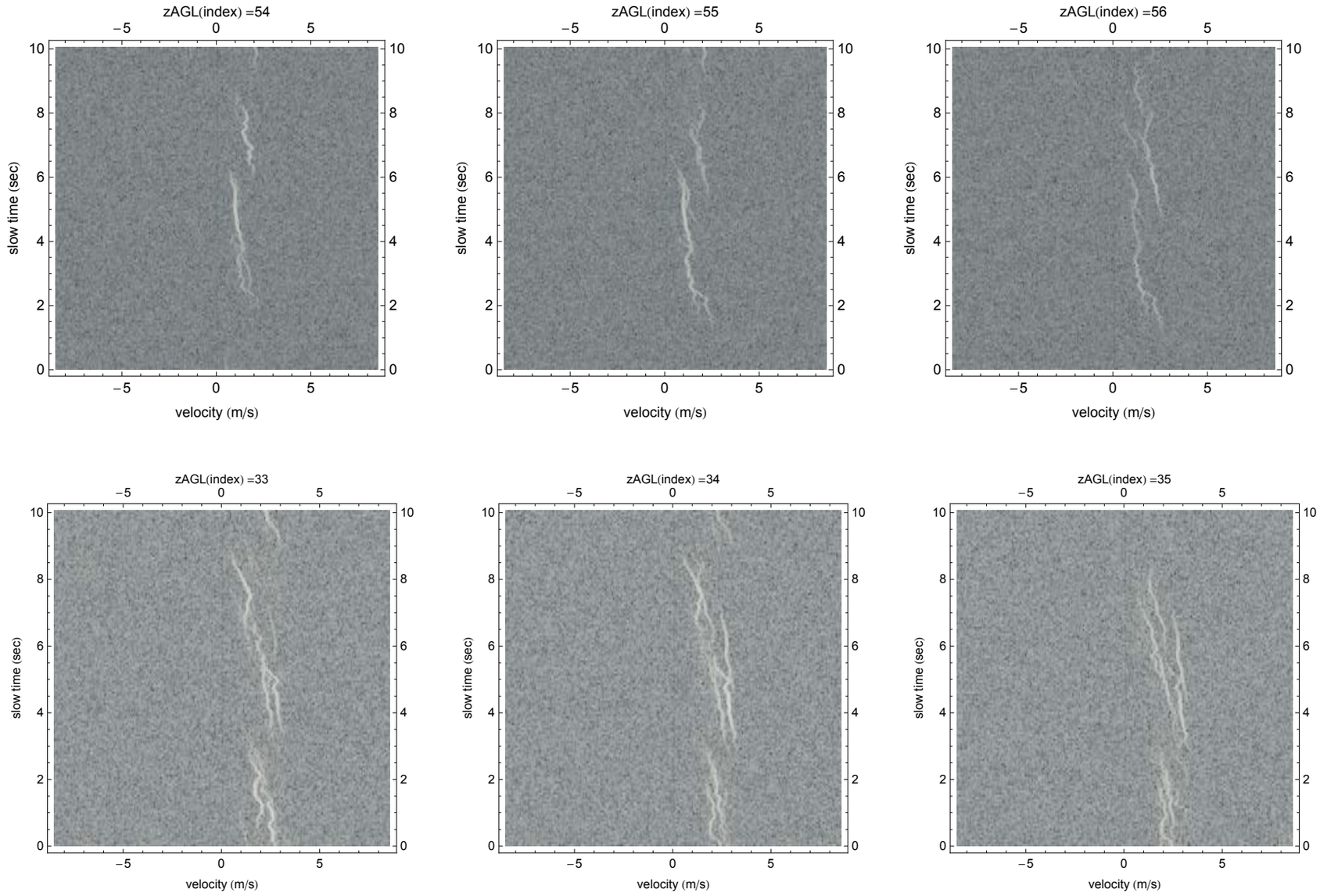

Figure 5. Observed vertical extent of echos from clear air contacts. This may simply be a direct result of spectral leakage,

The information necessary to support single radar beam wind speed and direction determination can be extracted from radar time-velocity grams using standard image processing techniques. This process is illustrated in figure 6. The upper left hand side of the figure 6 shows a time-velocity gram for the 34th range bin corresponding to an altitude of 142 m above ground level. The center portion of the figure shows the results of thresholding the image, forming clusters and rejecting clusters below a certain size threshold. In this case the signal to noise (SNR) threshold is 7 dB and the small component size is 20.

The lower right hand side of the figure illustrates the process of information extraction. The beginning and end points of each cluster respectively correspond to the velocity-time pairs (V_1, t_1) and (V_2, t_2). These locations together with

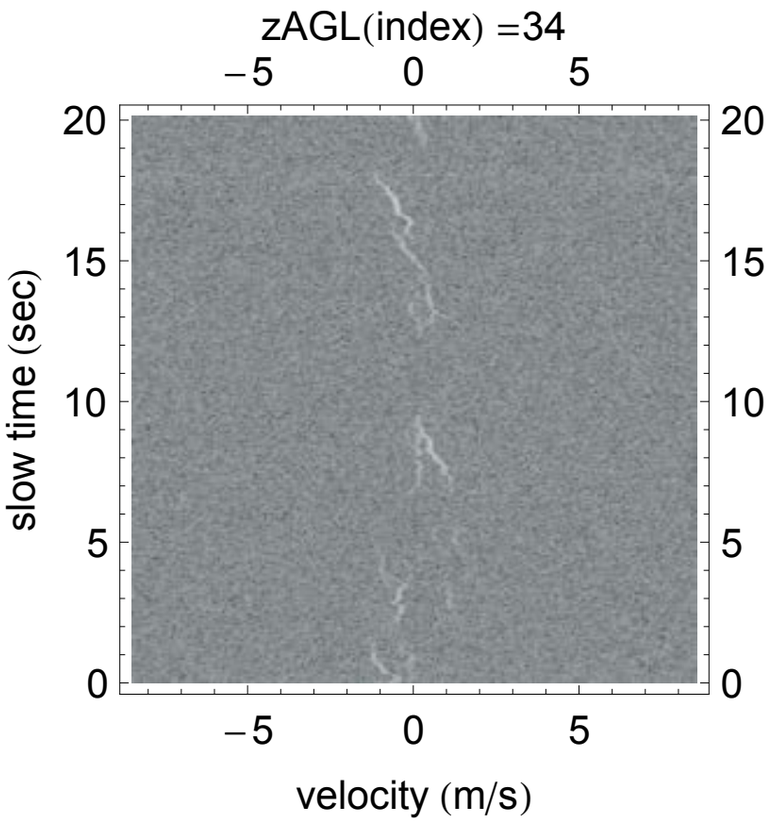

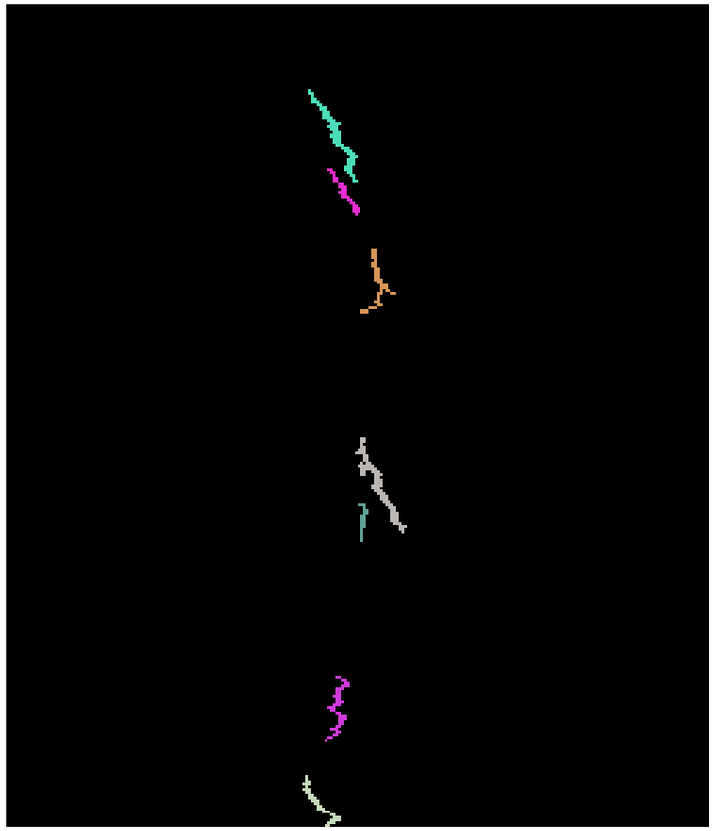

Figure 6. Image morphology and information extraction. Upper left) Image. Upper right) Connected morphological components. Lower) Identification of key times and Doppler velocities.

the location of the mid-crossing Doppler velocity $V = (V_1 + V_2)/2$ are illustrated in the lower right image. This process is repeated for each altitude bin where the radar can focus in order to build up a data set of accelerations and Dopplers from which wind speed and direction are determined. This is done in conjunction with the principle of least squares to select the wind speed and direction in an altitude band that is most consistent with the observed data in that altitude band. There is a definite art to this as there is to morphological image processing in general. In particular, morphological features that are inconsistent with the underlying single beam assumptions must be filtered out. Details of this are beyond the scope of this document.

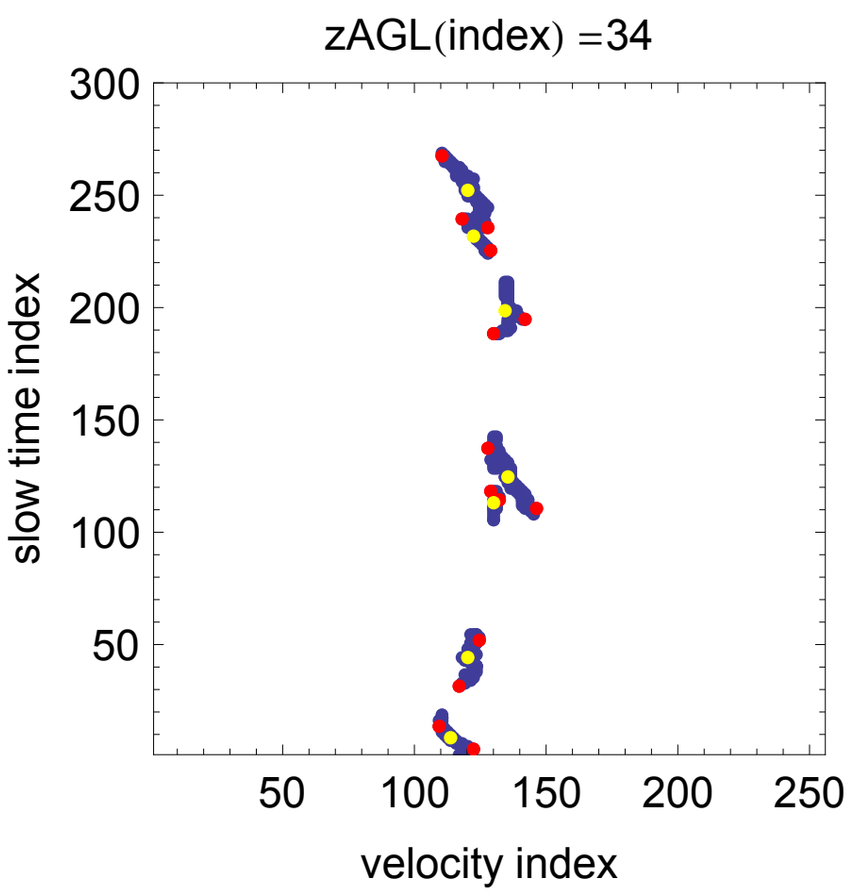

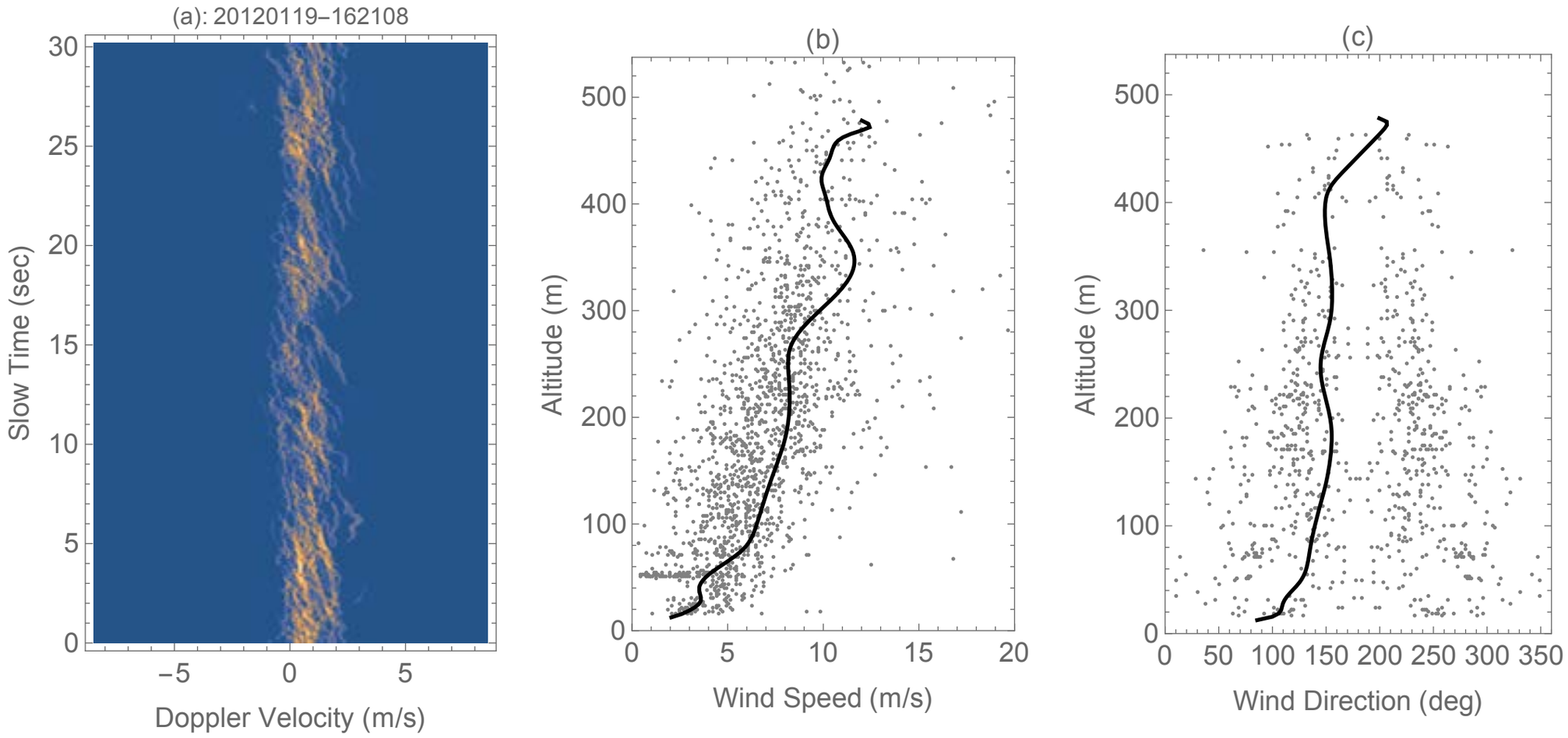

Figure 7. Single beam wind speed and direction compared to the Multi Beam Wind Engine model using data form Slidell, LA 19 January 2012.

The last two figures in this section compare wind speed and direction estimated using the single beam technique to wind velocity velocity measurements from a model that used beam data collected in the four cardinal directions. Wind direction at an altitude in the single beam approach is estimated from

$$\cos(\psi - \phi) = -\frac{V}{v\cos(\theta)}$$

where ψ is the unknown wind direction and ϕ is the known beam azimuthal direction and θ is the beam elevation angle, V is the observed Doppler velocity of the particle and v is the particle velocity computed as previously described. Solving for the wind angle ψ as previously shown leads to the two-branched solution

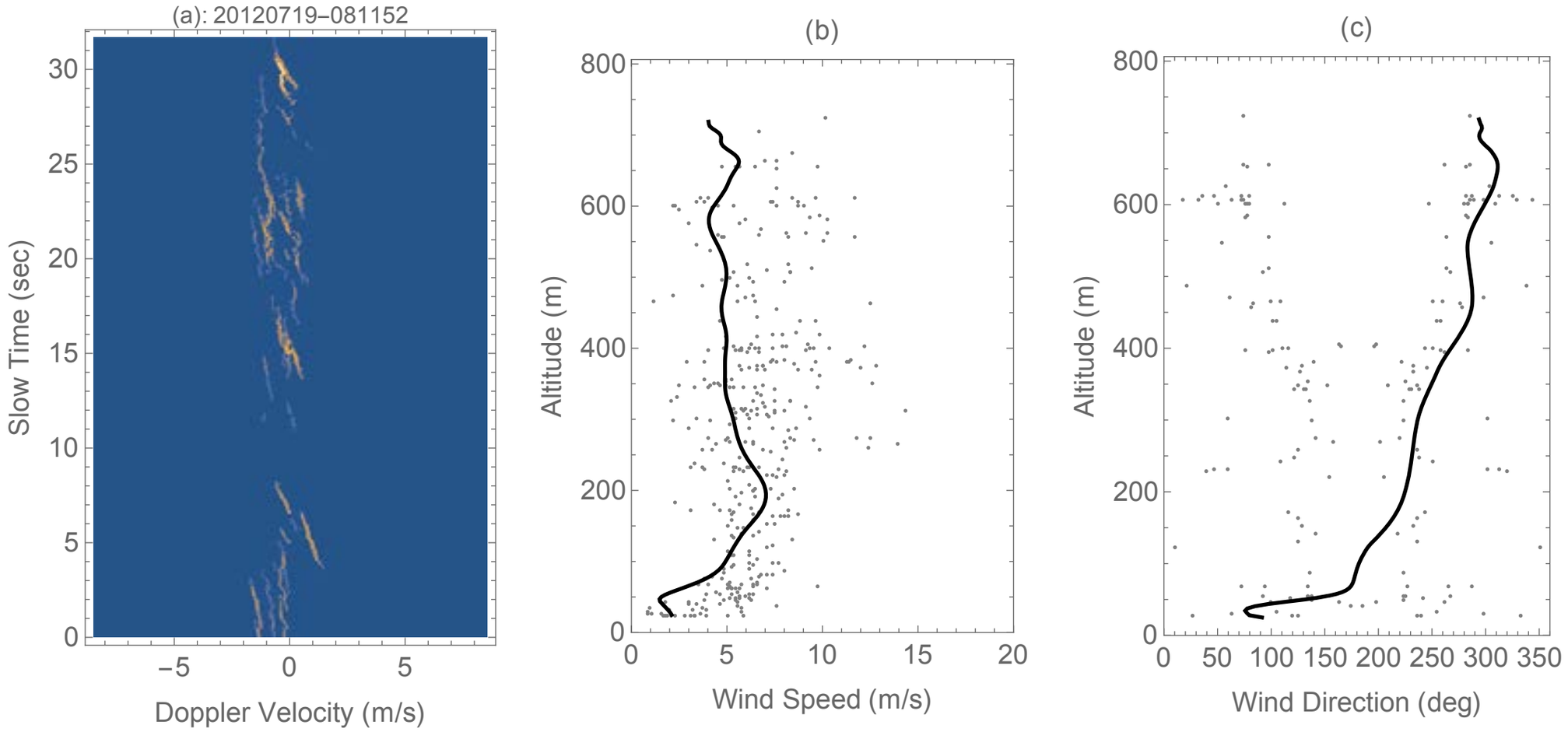

Figure 8. Single beam wind speed and direction compared to the Multi Beam Wind Engine model using data from Eloy, AZ 19 July 20212.

$$\psi = \phi \pm \arccos\left(-\frac{V}{v\cos(\theta)}\right)$$

This simply means that the single beam technique estimates wind direction relative to the radar beam pointing direction and cannot tell left from right due to the even nature of the cosine function.

The leftmost figure in each group shows the marginalization of the radar data cube across altitude at a fixed SNR threshold. Data are counts. It is presented for informational purposes only. The center figure shows the single beam wind speed estimates (points) compared to the Multi Beam Wind Engine model (thick black line). The right figure compares the single beam wind direction estimates (points) to MBWE (thick black line). Both branches of the wind direction estimate are presented for the

single beam technique. There is obviously a great deal of dispersion in the single beam estimates but overall agreement between the two approaches in these cases is quite good. We caution that the single beam approach would not be appropriate in a situation where it is raining or snowing. In these circumstances the particles that the radar tracks have a significant vertical component and the single beam technique is not applicable in its current form.

Estimation of Wind Velocity Using Only Particle Crossing Times

Introduction

In the previous section we presented a technique for estimating wind speed and direction based upon observations of the change in Doppler velocity as a turbulent wind particle crossed a WiPPR beam and the associated crossing time of the particle. In this section we present a method through which wind speed, but not direction, can be estimated through observation of only crossing particle times. The estimation technique is based on standard Bayesian probability theory and is easily doable from a computational standpoint because only a single parameter is estimated at each altitude, namely the wind speed v .

Background

During the spring and summer of 2012 the Wind Profiling Portable Radar (WiPPR) system was operated at a number of different sites in the deserts of the American Southwest. During the course of these operations it was consistently observed that the radar was able to track point-like objects associated with solar-driven convective turbulence. The tracks of these turbulent particles were resolved by the radar into time-Doppler velocity-altitude positions. Examples of some these data are shown in figure 1 left and 1 right. An important feature of these data is that the particles clearly enter and exit the radar beam at distinct times. Each of the particle tracks in these two figures is associated with a distinct altitude which varies little over the time history of the track. Said another way, the particles move primarily parallel to the ground. Since the width of the radar beam is a known quantity, the diameter of the radar beam at an altitude can be calculated by multiplying contact altitude by radar beam width. For the WiPPR system in 2012 the full beam width was approximately 6 deg. The fact that the crossing time of a particle and its maximum possible track length can be determined from the data suggest that it may be possible to estimate wind speed without using Doppler velocity. This document presents a Bayesian statistical technique for accomplishing this task.

Discussion

First we affix our geometry and notation. We consider a near vertical radar beam of linear width $2a$ at an altitude z above ground level as shown in figure 2. If $d\theta$ denotes the angular beam width of the radar beam then $2a = z\sin(d\theta)$. A turbulent particle moving parallel to the ground enters the beam at a point A and exits the beam at point B. The particle's closest point of approach to the beam center is denoted by y. The points A and B are respectively located at points $((a^2 - y^2)^{1/2}, y)$ and $(-(a^2 - y^2)^{1/2}, y)$. The length of the particle's track within the radar beam is $2(a^2 - y^2)^{1/2}$. We will assume that the closest point of approach is uniformly distributed on the interval $(-a, a)$.

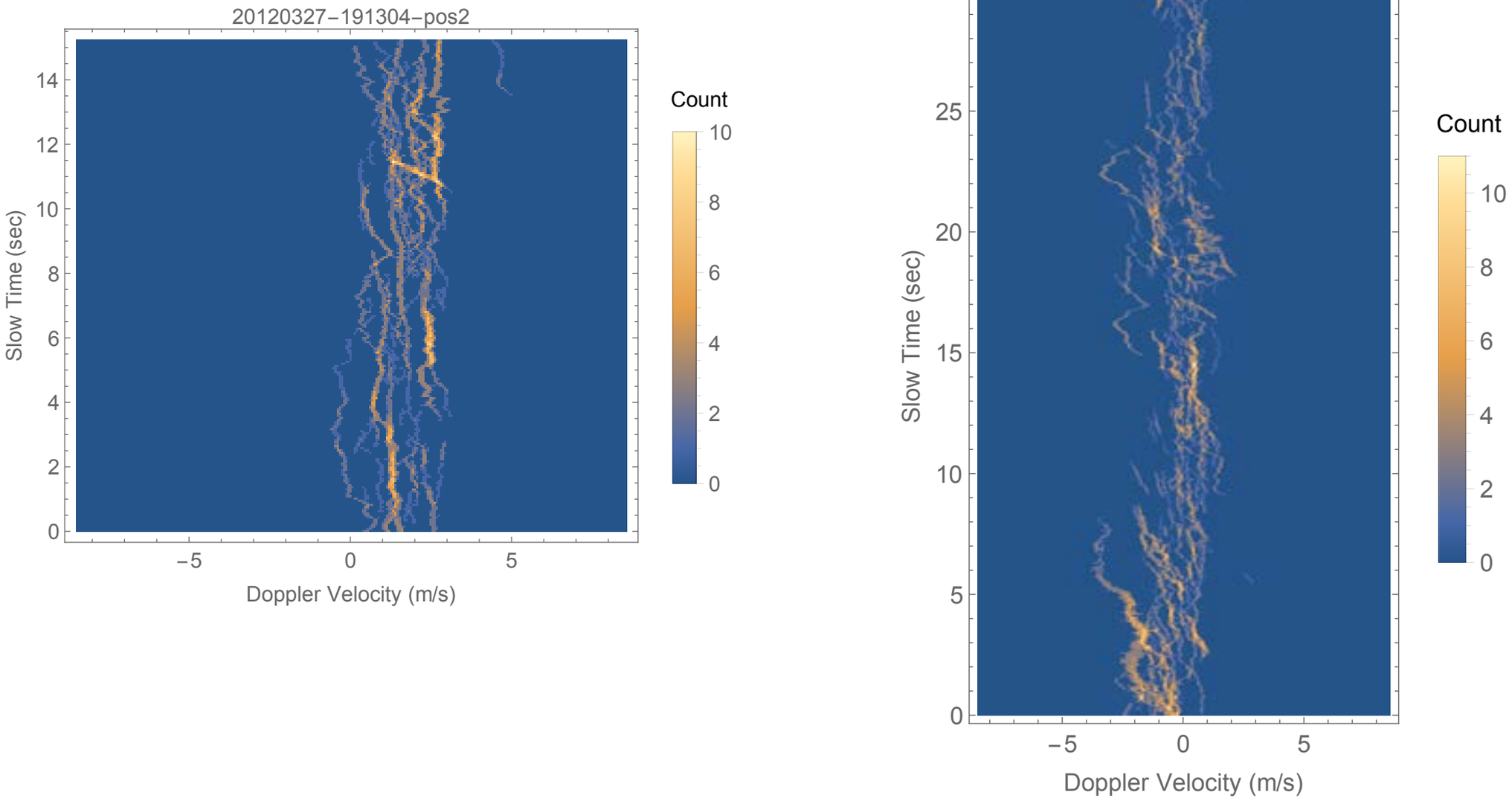

Figure 1. Left) Observed turbulent particle crossing times on the WPPR system from 27 March 2012 in the Cibola desert north of Yuma AZ. Right) Observed turbulent particle crossing times on the WPPR system from 11 September 2012 near Granite Peak on the Dugway proving Grounds UT

Additionally we assume N particle crossings with crossing times $(t_1, t_2, \ldots t_N)$ are observed by the radar. Assuming that each particle is moving with constant speed v, then how do we determine v from the observed crossing times?

If both the particle velocity v and it closest point of approach y_n were known then the crossing-time data would satisfy

$$t_n = 2(a^2 - y_n^2)^{1/2}/v$$

for $-a < y_n < a$. If we denote the observed crossing time data by D, then Bayes theorem tells us that

$$P(v \mid D) = \frac{P(v)L(D \mid v)}{P(D)}$$

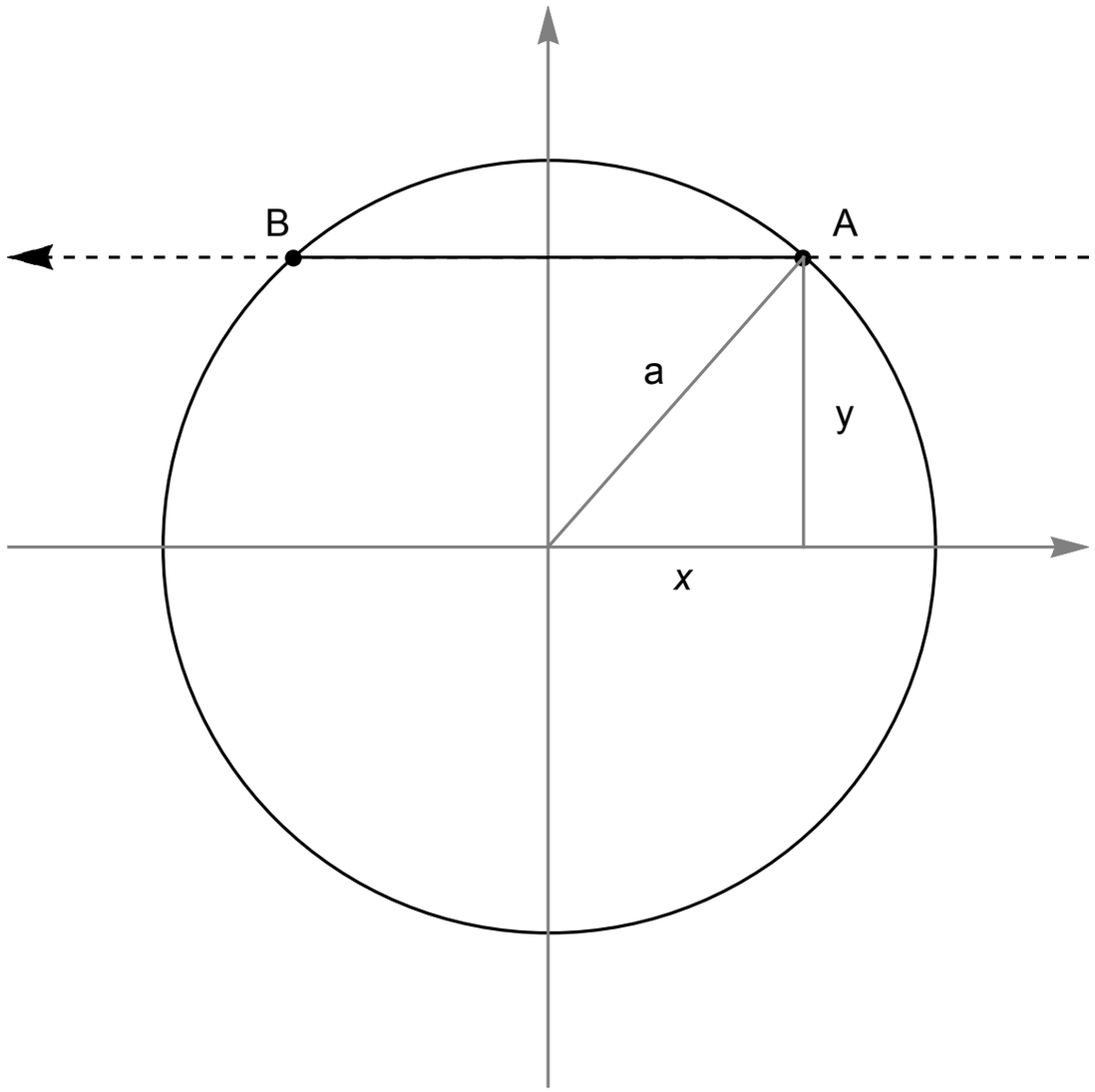

Figure 2. Particle-beam crossing geometry. The view is from above the radar beam looking down. the diameter of the radar beam at the altitude of the particle is 2a. The turbulent particle enters the beam at point A and exits the beam at point B.

where $P(v \mid D)$ is the posterior probability distribution of wind speed v given the observed data D, $L(D \mid v)$is the likelihood of the observed data given wind speed v, $P(v)$ is the prior probability density of wind speed and $P(D)$ is the evidence . Since the particle closest point of approach is a random quantity it follows that particle crossing time is a random quantity as well. If we let $f(t \mid v)$ denote the probability density function of crossing time given the wind speed v, then the likelihood of the observed crossing time data is

$$L(D \mid v) = \prod_{n=1}^{N} f(t_n \mid v)$$

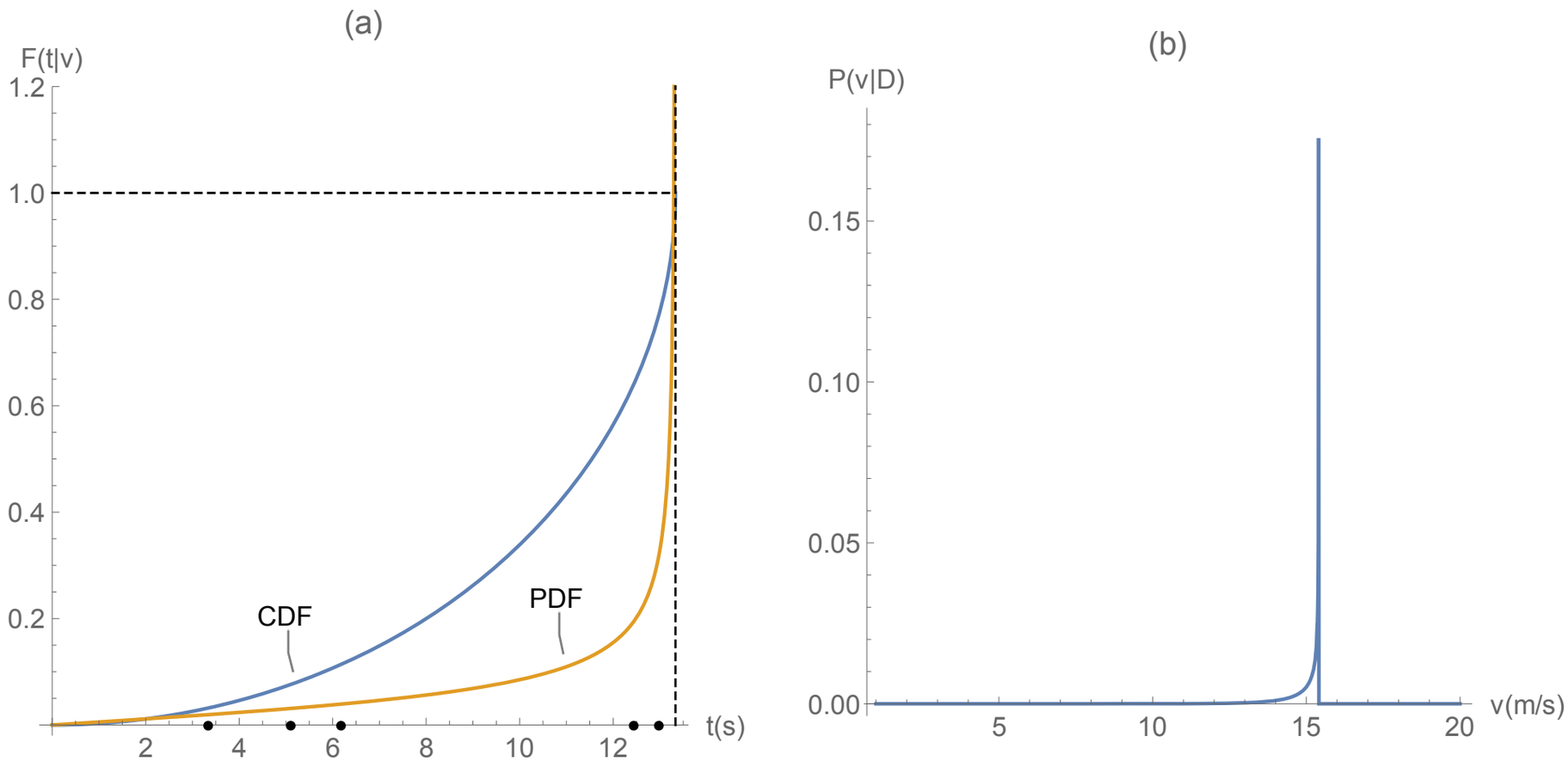

Figure 3. (a) Cumulative probability density and probability density of particle crossing time for a radar beam with a 100 m radius and 15.0 m/s wind speed. (b) Posterior probability density of wind speed based upon simulated crossing times D={3.33604 s,12.9862 s,6.16756 s,5.11693 s,12.4246 s}. The location of the data points are indicated by the black dots in part (a). The probability density function f(t|v) has a one over square root singularity at t=2a/v. This is indicated by the vertical dashed line in part (a). The horizontal dashed line in (a) is the upper limit of the CDF.

The likelihood function $L(D \mid v)$ is a probability density function with respect to the data samples t_n but it is not a probability density function with respect to the unknown parameter v, wind speed.

In problems of parameter estimation the evidence $P(D)$ acts only as a normalization constant. Specifically it is

$$P(D) = \int_0^{v_{max}} L(D \mid v) P(v) dv$$

If we have no prior knowledge of wind speed then the sensible thing to do is to assume a flat prior, i.e. $P(v)$ proportional to a constant. If we assume a flat prior on the interval $(0, v_{max})$ then

$P(v) = v_{max}^{-1}$ on this interval. In this case the posterior probability density apart from normalization is equal to the likelihood:

$$P(v \mid D) = C_0 \prod_{n=1}^{N} f(t_n \mid v)$$

where C_0 is a normalization constant that can be found by requiring $P(v \mid D)$ to be a probability density function.

In order to compute the likelihood of the data (and hence the posterior probability of wind speed) we need to know the probability density function for particle crossing time as a function of wind speed v. This can be obtained by first finding the cumulative probability density function $F(t \mid v)$ of particle crossing time and then differentiating to obtain the desired probability density function $f(t \mid v)$. By definition the cumulative probability density function $F(t \mid v) = Pr(T < t)$ where the symbol Pr denotes probability, T denotes the random variable crossing time and t is a specific value of that random variable. The principle of marginalization allows us to write

$$F(t \mid v) = \frac{1}{2} Pr(T < t \mid Y > 0) + \frac{1}{2} Pr(T < t \mid Y < 0)$$

where Y denotes the random variable closest point of approach. Using the fact that crossing time and closest point of approach are related by $T = 2(a^2 - Y^2)^{1/2}/v$ and the fact that the random variable Y is uniformly distributed on$(-a, a)$ leads to

$$Pr(T < t \mid Y > 0) = Pr(Y > (a^2 - (vt/2)^2)^{1/2}) =$$

$$\frac{1}{a} \int_{(a^2-(vt/2)^2)^{1/2}}^{a} da = \frac{a - (a^2 - (vt/2)^{1/2})^{1/2}}{a}$$

provided $0 < vt/2 < a$. By symmetry the probabilities $Pr(T < t \mid Y > 0)$ and $Pr(T < t \mid Y < 0)$ are equal. Thus it is the case that the cumulative distribution function of particle crossing time is given by

$$F(t \mid v) = \frac{a - (a^2 - (vt/2)^{1/2})^{1/2}}{a}$$

provided $0 < t < 2a/v$ and zero otherwise. Differentiating the cumulative probability density function $F(t \mid v)$ to obtain $f(t \mid v)$ gives

$$f(t \mid v) = \frac{v^2 t}{4a(a^2 - (vt/2)^2)^{1/2}}$$

provided $0 < t < 2a/v$ and zero otherwise.

Once $f(t \mid v)$ is known the likelihood of the data as a function of wind speed can be computed. Wind speed can then be estimated by choosing the wind speed that maximizes the likelihood of the data. Alternatively one can compute the mean of the posterior probability distribution. In specific terms this is

$$E(v) = \frac{\int_0^{v_{max}} L(D \mid v) dv}{\int_0^{v_{max}} v L(D \mid v) dv}$$

where E denotes expected value and $L(D \mid v) = \prod_{n=1}^{N} f(t_n \mid v)$ and v_{max} is a rough estimate of the maximum possible wind speed based upon a priori knowledge. For a large number of data samples, i.e. large N, the likelihood function is a very sharp peaked function of v and the choice of v_{max} does not influence our results in any material way.

Computations

An illustration of estimating wind velocity by the maximum likelihood technique using a synthetic data set is presented in figure 3. The radius of the radar beam spot a and the wind velocity v are respectively assumed to be 100 m and 15 m/s. A random number generator has been used to generate five points of closest particle approach to the radar beam center on the interval $(-a < y < a)$. Five particle crossing times were then computed using $t_n = 2(a^2 - y_n^2)^{1/2}/v$. Part (a) of the figure shows the cumulative density function (CDF) and the probability density function (PDF) of the random variable crossing time. The PDF $f(t \mid v)$ has an integrable singularity at $t = 2a/v$ as indicated by the vertical dashed line in part (a). Part (b) of the figure shows the numerical computation of the likelihood function $L(D \mid v)$ over the velocity range $0<v<20$ m/s. $L(D \mid v)$ is clearly peaked at v =15 m/s. As is often the case, the Bayesian approach produces a very common sense result. As indicated in the figure caption, the slowest particle crossing time in the synthetic data set was approximately 13 s. The slowest crossing time is the crossing time of the particle track that has the closest point of approach to the beam center. A reasonable guess as to the particle path length in the radar beam for this particle is the beam diameter $2a$ and the corresponding wind speed estimate becomes $v = 2 * 100/13 = 15.4$ m/s.

A wind speed profile estimate using actual measured data is shown in figure 4. Part (a) shows the observed particle crossing times observed over approximately 80 seconds of clock time. Part (b) of the figure compares the crossing time only estimate to an estimate using measured Doppler velocity in multiple look directions. The agreement is quite good especially near the ground.

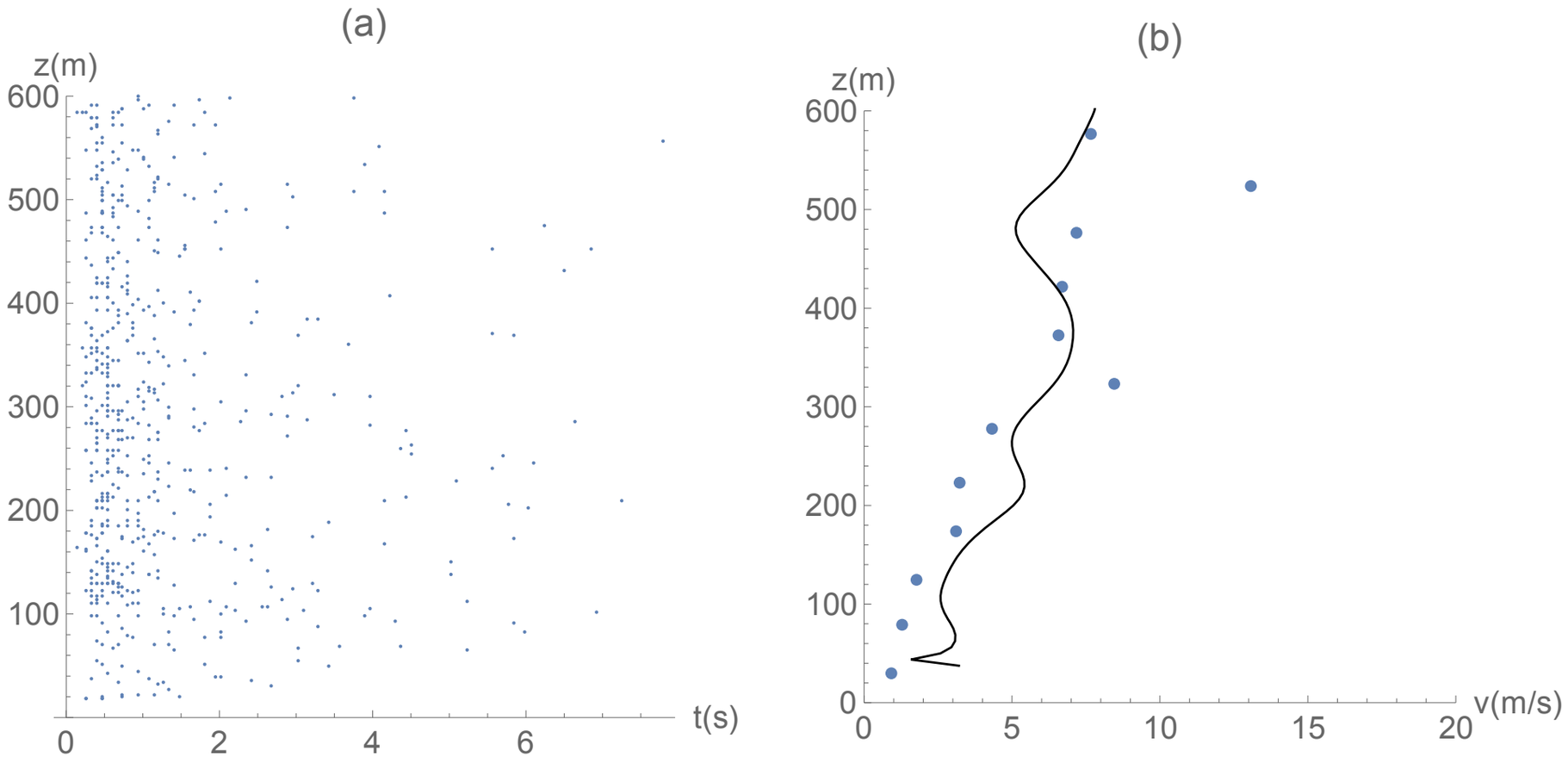

Figure 4. (a) Observed turbulent particle crossing times on 27 March 2012 in the Cibola desert north of Yuma AZ. (b) Estimated wind speed from the crossing time data (points) compared to a WiPPR wind speed estimate using Doppler data (line). The crossing time data have been grouped into altitude bins of 50 m height in order to support the crossing-time only estimate of wind speed.

Revolving Single Beam Inversion

The previous two sections have focused on techniques that employ a single, fixed non-rotating radar beam. This is in contrast to the standard WiPRR technique involving 4 beams oriented in the cardinal directions.

Wind speed and direction can be also be measured by WiPPR using a single radar beam that continuously rotates in azimuth. This produces a simpler system mechanical structure and simpler data processing. The simplification in data processing comes with the higher price of needing to record real time FMCW radar data. There is also the possibility of loss in SNR due to lack of averaging across slow time. Normally in WiPPR processing 160-200 range velocity matrices are averaged together in order to reduce the variance of the noise in Doppler velocity-slant range cells. This is not possible in the single beam approaches described here. This is because the single beam approaches rely on tracking the behavior of particles in time. Thus averaging across time is not possible or appropriate.

The revolving beam inversion is accomplished by detecting the the time variation of the Doppler velocity of turbulent clear air scatter particles as they move through the time-altitude-velocity data cube of the radar. To better understand this process we begin by looking at a fixed beam data cube.

An example of such a radar data cube for a non-moving, single-beam radar configuration is shown in figure 1a. These data were recorded on 27 March 2013 at Yuma, AZ. The radar beam was pointed to the west. The sweep width of the radar was set to $B =$ 24 MHz and the pulse length of the radar was $T_m = 262.144$ msec. The 24 MHz sweep width produces slant range cells that that are 6.25 m in slant range extent ($dr = c/2B$). The radar data cube extends from 0-800 m in altitude, from -8.6 to 8.6 m/s in Doppler velocity and from 0-26 sec in time. As can be seen from the figure, the radar resolves the echos from turbulence into particle like tracks.

Figure 1b shows the marginalization of the radar data cube across altitude. This has been accomplished by thresholding at a SNR level of 15 dB. Any voxel with SNR greater than 15 dB has been set to 1. All remaining voxels are set to zero. The data cube is then summed across altitude in order to produce a two dimensional figure. Data values in figure 1b are counts. This process discards altitude information but makes for easier physical interpretation. The slow time scale shown in figure 1b is measured in time steps equal to the pulse length T_m. The Doppler

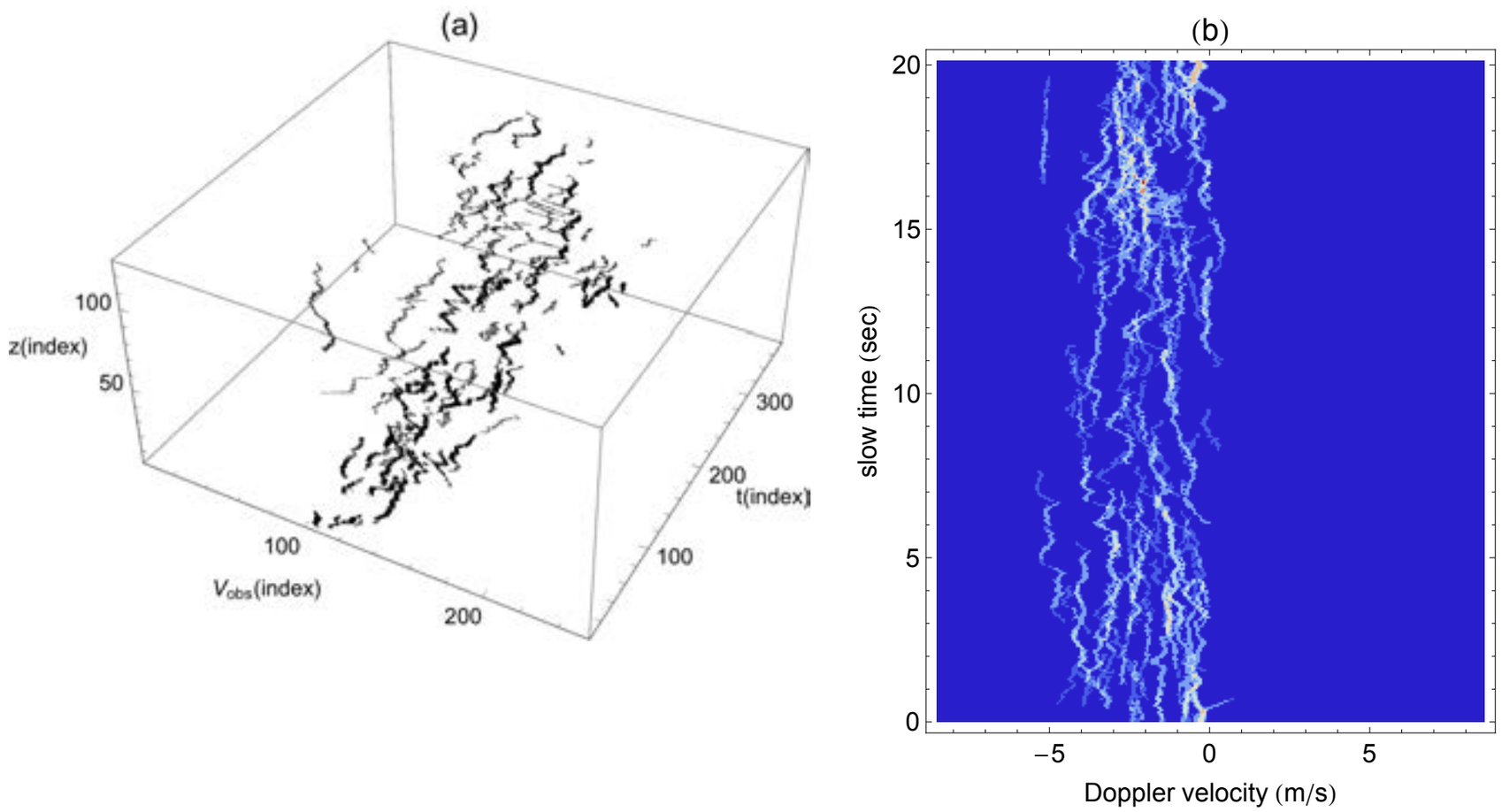

Figure 1. Radar data cube for 27 March 2012 for a fixed, non-moving radar beam at an elevation angle of 80 deg.

range in figure 1b is $(-\lambda/4T_m, \lambda/4T_m)$ where λ is the wavelength corresponding to the carrier frequency of the radar.

The particle character of the data is clearly evident in figure 1b. The wavy nature of the curves in figure 1b is caused by the acceleration and de-acceleration of the turbulence during the time period when it was in the radar beam. If the particles were ideal and moving with constant velocity then figure 1b would consist of straight line tracks with a slope to the left.

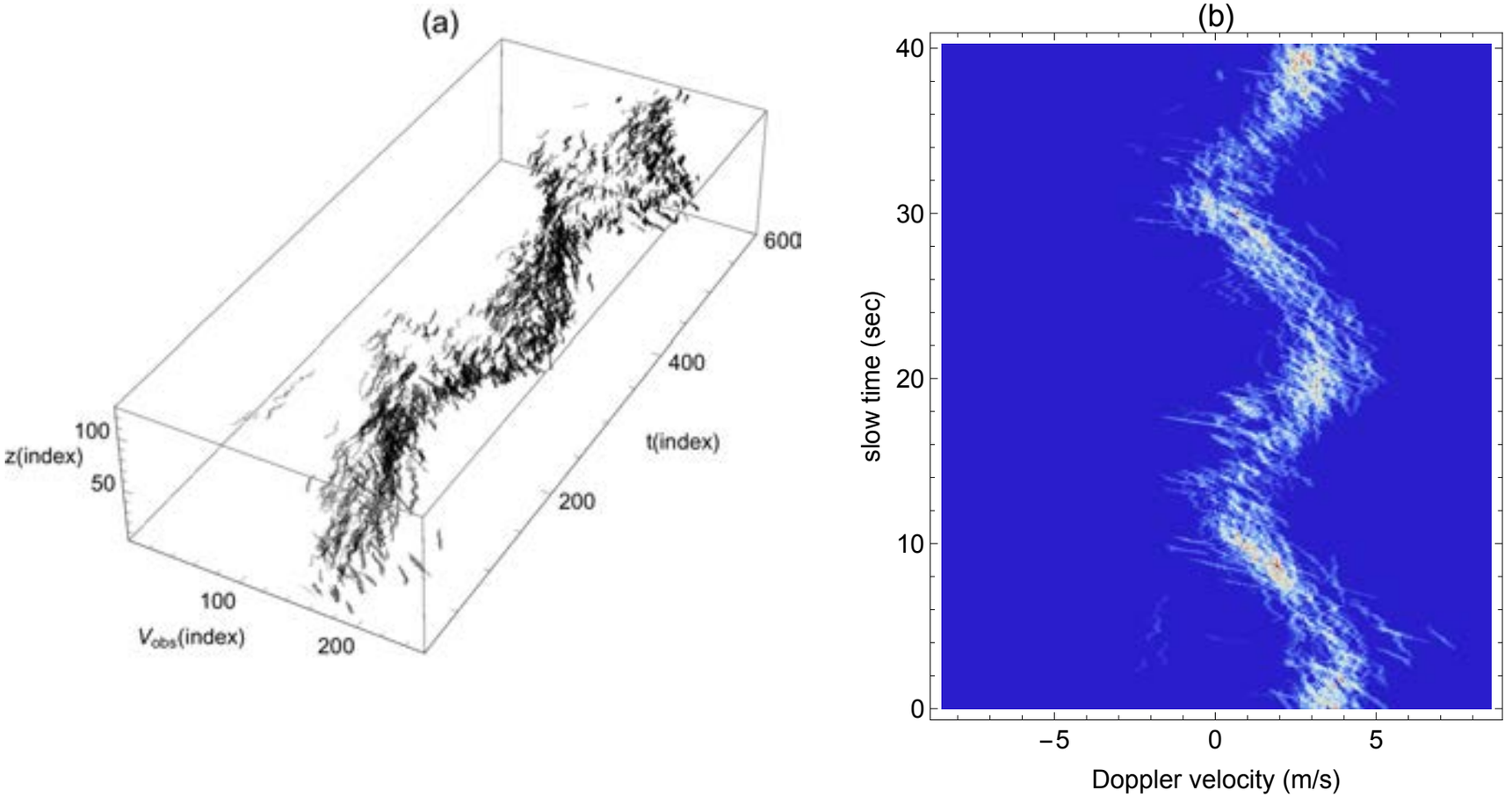

Figure 2. Radar data cube for 23 March 2012 for a rotating radar beam at an elevation angle of 80 deg.

A radar data cube for data collected on 23 March 2012 during a time period in which the radar was slowly rotating in a clockwise sense is shown in figure 2a. The marginalization across altitude for the data cube is shown in figure 2b. These data were collected with a 36 MHz sweep width. The dimensions of the radar data cube are 0-533 m in altitude, -8.6-8.6 m/s in Doppler velocity and 0-40 sec in time. As can be seen by examining the figure, the Doppler velocity has a sine-like character as a function of time. This is caused by the fact that the radar beam is rotating at a constant angular velocity and thereby causing a smooth transition between maximum and minimum Doppler velocity. When the radar beam is pointed into the wind maximal values of Doppler are observed. When the radar beam is pointed in the opposite direction minimal values of Doppler are observed.

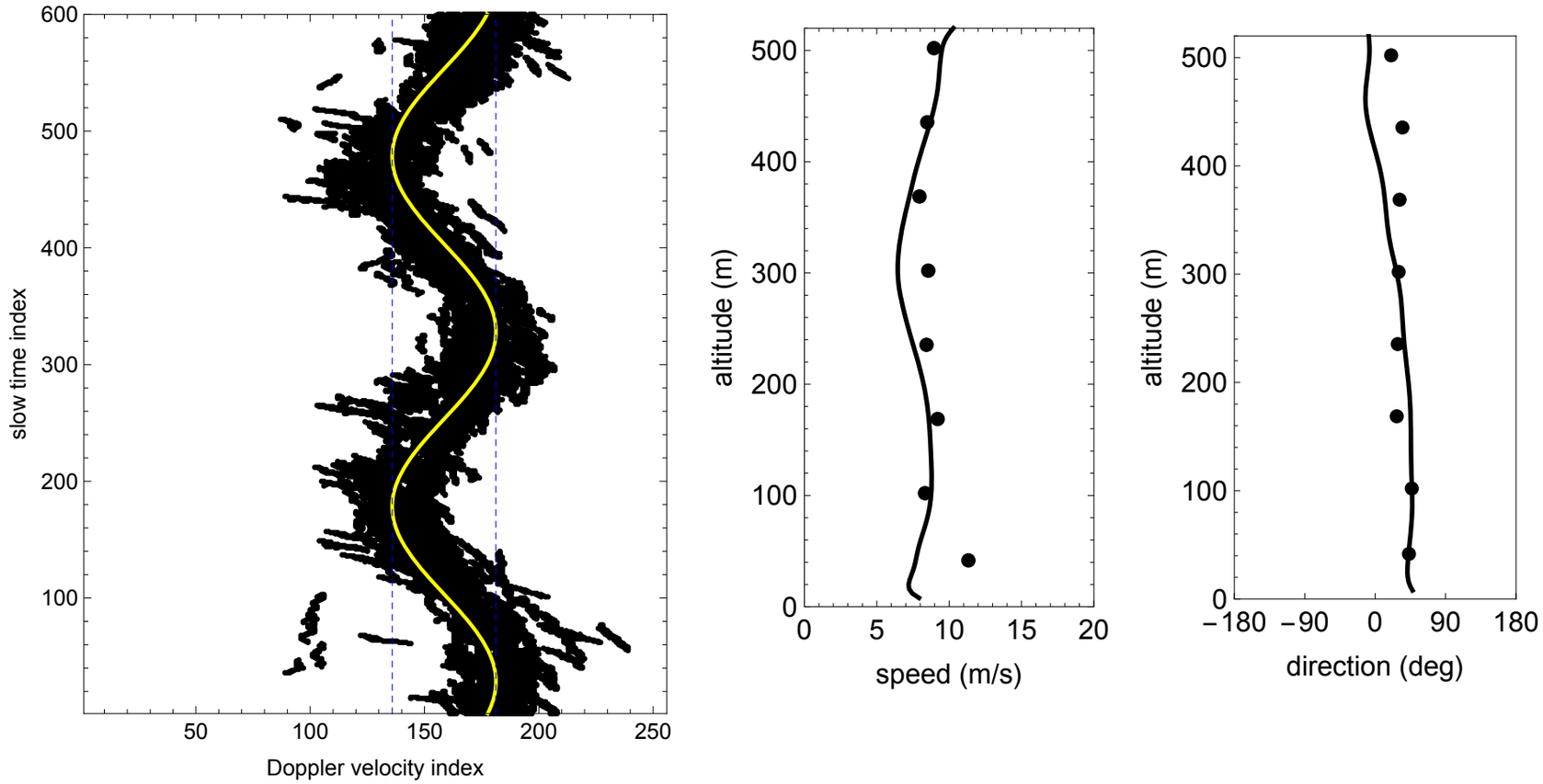

Figure 3. Estimation of wind speed and direction from rotating beam radar data. Left) Yellow cure is a fit of a sinusoidal function with an offset to the observe data. Right) Revolving beam estimates (points) compared to another estimate of wind speed and direction.

The observed variation in Doppler velocity is of the form

$$V(t) = V_0 + V_m \cos[2\pi(t + T_0)/T]$$

where t is time, T is the period of revolution of the radar beam and $2\pi T_0/T$ is a phase angle related to the direction of the wind.

The maximum and minimum Doppler shift that the radar sees are

$$(V_{min}, V_{max}) = (V_0 - V_m, V_0 + V_m).$$

The direction of the wind can be found by identifying the time at which maximum Doppler occurs in $V(t)$ and relating that time to

the corresponding azimuthal pointing-direction of the beam. The wind speed v is given by the equation

$$v = \frac{V_{max} - V_{min}}{2\cos\theta} = \frac{V_m}{\cos(\theta)}$$

where θ is the elevation angle of the radar beam from the horizontal. The position of (V_{min}, V_{max}) relative to the fitted cosine wave $V(t)$ are indicated by the vertical lines in figure 3 left side.

Wind speed and direction as a function of altitude can be found by subdividing the radar data cube into multiple altitude ranges and making speed-direction estimates for each altitude band using the above described procedure. The result of doing this is shown in figure 3 right side. The radar cube has been divided into 8 altitude bins (ranges). Estimated speed and wind direction values are compared in the figure to speed and wind direction values made using an independent measurement technique.

A somewhat more theoretical take on the revolving beam approach is as follows. Suppose that the azimuthal angle of the radar beam pointing direction is given by

$$\phi(t) = 2\pi\cos(2\pi t/T)$$

where T is the period of revolution. At times $(0, \frac{T}{4}, \frac{T}{2}, \frac{3T}{4})$ the beam points in the directions (N,E,S,W). Additionally suppose that the wind is coming from angle ψ with speed v and that the particles in the wind are falling with speed $v_{fall} > 0$. The vector velocity of these particles is

$$\mathbf{v}_{wind} = (v\sin(\psi), v\cos(\psi), -v_{fall})$$

The instantaneous pointing direction of the radar beam is

$$\boldsymbol{\eta}_{beam}(t) = (\sin[\phi(t)]\cos(\theta), \cos[\phi(t)]\cos(\theta), \sin(\theta))$$

And the Doppler shift is $V(t) = -\boldsymbol{\eta}_{beam}(t) \,.\, \boldsymbol{v}_{wind}$ which is

$$V(t) = -v\cos(\theta)\cos[\psi - \phi(t)] + v_{fall}\sin(\theta)$$

So the variation in Doppler is centered on $V_0 = v_{fall}\sin(\theta)$ with maximum variation $V_m = v\cos(\theta)$. These can readily be determined by simple signal processing techniques.

Thus the rotating beam technique will work with clear air scatter or during times when hydrometers are falling (rain or snow). The technique will not work in cases when the revolving radar beam does not see the falling hydrometers in all directions. This is usually the case with virga which is typically very spatially variable.